Brain Research, 543 (1991) 36–44
Elsevier

BRES 16389

Vestibular afferent responses to microrotational stimuli

Steven F. Myers[1] and Edwin R. Lewis[2]

[1]*Department of Otolaryngology, 5E-UHC, Wayne State University School of Medicine, Detroit, MI 48201 (U.S.A.) and* [2]*Department of Electrical Engineering and Computer Sciences, University of California, Berkeley, CA 94720 (U.S.A.)*

(Accepted 25 September 1990)

Key words: Semicircular canal; Utricle; Utricular afferent neuron; Striola; Jerk sensor; Lucifer yellow

Intracellular microelectrode recording/labelling techniques were used to investigate vestibular afferent responses in the bullfrog, to very small amplitude (<0.5° p–p) sinusoidal rotations in the vertical plane over the frequency range of 0.063–4 Hz. The axis of rotation was congruent with the axis of the anterior semicircular canal. Robust responses to peak accelerations as low as 0.031°/s^2 were obtained from units subsequently traced to either the central portion of the anterior canal crista or the striolar region of the utricle. All of these microrotationally sensitive afferent neurons had irregular resting discharge rates and the majority had transfer ratios (relative to rotational velocity) of 1–40 spikes/s per degree/s. Individual utricular afferent velocity transfer ratios were nearly constant over the frequency range of 0.125–4 Hz. Canal units generally displayed decreasing response transfer ratios as stimulus frequencies increased. These findings indicate that although utricular striolar and central crista afferent velocity transfer ratios to microrotations were very similar, utricular striolar afferent neurons were more faithful sensors of very small amplitude rotational velocity in the vertical plane.

INTRODUCTION

The vestibular system is capable of sensing extremely small rotational accelerations. The vestibulo–ocular reflex (VOR) has been shown to respond to peak sinusoidal accelerations down to at least 0.04°/s^2 with angular displacements of 0.04 degrees peak to peak (p–p)[15,19]. However, very little is known about the operation of the vestibular sensors themselves in response to such very small amplitude stimuli. Previous researchers have used much larger amplitudes, seldom below 10° p–p, in their studies of vestibular afferent responses. Based on findings from some of these studies, a threshold (absolute minimum detectable) rotational stimulus was proposed for vestibular afferent axons, and estimated to be approximately 0.2°/s^2 for both amphibians and mammals[14,16]. Other investigators (e.g. Lowenstein[10]) have proposed that there is no true vestibular threshold in axons with non-zero resting spike rates, and that noise imposes the only limits on the amplitudes of detectable stimuli.

The current study was undertaken to provide quantitative information on the responsiveness of vestibular afferent neurons to rotational stimuli with amplitudes of acceleration at or below 0.2°/s^2.

MATERIALS AND METHODS

Bullfrogs (*Rana catesbeiana*) weighing 50–180 g were anesthetized with either sodium pentobarbital alone (60 μg/g body weight i.m.) or in combination with ketamine hydrochloride (30 μg/g of each anesthetic) with supplemental injections as necessary. During surgery and throughout the physiological experiment, the frog was covered with damp gauze to facilitate cutaneous respiration. The VIIIth nerve was approached through the roof of the mouth by the removal of a small patch of mucosa, drilling through the underlying bone and cartilage with a dental drill to expose the dura directly over the VIIIth nerve in the cranial cavity (the otic capsule remaining intact), and careful removal of the dura overlying the nerve. The frog was then positioned ventral side up on a servo motor-driven tilt table with the axis of the anterior vertical canal congruent with the axis of tilting motion (rotation in the vertical plane; see Fig. 1). Applied stimuli comprised sinusoidal tilts of 0.05–1.6° p–p with frequencies ranging from 0.063 to 4 Hz. The plane of the utricle was approximately horizontal at the sinusoidal zero-crossings of the table motion and within 3 mm of the axis of rotation.

The activity of single vestibular nerve fibers was recorded intra-axonally with single-barrelled glass micropipettes. Electrode tips were filled by capillary action with a 5% (w/w) solution of the fluorescent dye Lucifer yellow[18] in distilled water and the shanks filled with a 5% (w/w) solution of Procion red in distilled water. The electrodes were inserted into a plastic holder containing a 0.5 M KCl solution and a Ag/AgCl pellet attached to a silver wire lead. The indifferent electrode comprised a plastic Petri dish filled with an agar gel made from 0.5 M KCl, with a second Ag/AgCl pellet embedded in the agar. The moist surface of the agar was kept in contact with the animal's skin.

Microelectrodes were visually positioned under low magnification

Correspondence: S.F. Myers, Department of Otolaryngology, 5E-UHC, Wayne State University School of Medicine, 540 East Canfield, Detroit, MI 48201, U.S.A.

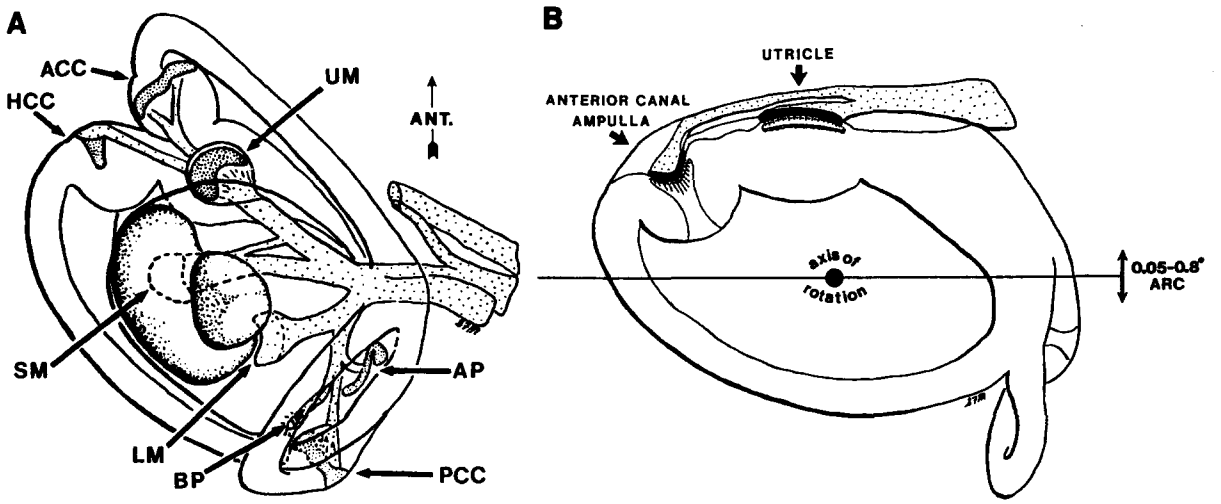

Fig. 1. A: illustration of bullfrog labyrinth (dorsal view). B: illustration showing orientation of labyrinth to the axis of rotation. The line through the axis of rotation represents the horizontal plane of the tilt-table.

and remotely advanced via a hydraulic microdrive into the anterior portion of the VIIIth nerve root proximal to the nerve ganglia. Electrode impedances ranged from 50–100 MΩ. Before the electrode was advanced into the nerve, a backing voltage of +40 mV was applied. A search stimulus of 0.4° p–p sinusoidal tilt at 0.5 Hz was used while the electrode was being advanced. If a penetrated axon's spike activity did not obviously follow the search stimulus, the amplitude of the stimulus would be increased to 1.6° p–p. When a responding unit was identified, the stimulus was turned off and 2 min of resting activity recorded on an FM cassette tape recorder capable of recording both spike activity and DC table position from a high-resolution potentiometer. A third channel on the tape recorder was used to record a sync pulse from a function generator that provided the drive signal for the servo motor controller. This sync pulse record for each unit was calibrated to the table position potentiometer record for each stimulus frequency and used to provide a precise reference point for determining afferent response phase relative to table position.

After 2 min of resting activity, recording of spike activity continued as sinusoidal steady-state stimuli were applied for approximately 2 min at each frequency. Approximately one-third of the single units were held long enough to record at 4 or more frequencies along with additional periods of resting activity. Stimulus frequencies applied included 0.063, 0.125, 0.25, 0.5, 1, 2, 4 and 8 Hz. Stimulus amplitudes (0.8–0.05° p–p) were adjusted at each frequency to obtain non-saturating responses (i.e. so that the negative portion of the stimulus modulation of spike rate was not clipped; the spike rate was not driven to zero at any part of the stimulus cycle). In many cases this was not possible due to the low resting spike rates of some units. For amplitudes less than 0.05°, distortion in the stimulus wave form was greater than 5% and therefore amplitudes in that range were not used.

During recording of neural activity, the backing voltage on the electrode was often removed. In many cases this was sufficient to successfully label the penetrated axon with Lucifer yellow. Active iontophoretic injection of Lucifer yellow was applied at the end of a recording session whenever possible by passage of a negative 3 nA p–p sinusoid superimposed on a negative 1.5 nA DC current. After dye injection, the backing voltage was applied again and the electrode withdrawn from the nerve. In most cases only one dye-fill was attempted per animal. However it eventually became routine practice for a second pass of the electrode to be made at a new location unambiguously distinguishable friom the first.

At the end of each experiment, the anesthetized animal was decapitated, the otic capsule opened with rongeurs and the head immersed in a 10% formalin solution containing 0.1 M sodium phosphate buffer, pH 7.3. After 48 h of fixation at room temperature, the VIIIth nerve and sensory endorgans were dissected in fresh buffer, dehydrated in graded ethanol series and cleared in methyl salicylate. Cleared tissue was mounted in depression slides containing methyl salicylate and examined with a Zeiss Universal microscope with fluorescence attachments. Incident illumination was provided by a mercury vapor lamp filtered through a 10 nm band-pass filter centered at 434.8 nm (PTR Optics). The axons and terminal arborizations of dye-filled afferent neurons were sketched against an eyepiece graticle and photographed with Ektachrome ASA 200 film. Axonal diameter measurements of the fluorescent dye-filled neurons represent internal axonal diameters and were made directly from the microscope using the calibrated eyepiece graticle and/or from the Ektachrome photographs using complementary photographs of a microscope-slide mounted micrometer.

Physiological data analysis was carried out on Compupro and IBM PC-AT microcomputers. Stimulus wave forms and neuronal response records were translated by comparator/Schmitt-trigger circuits into two series of pulses, carried over two lines to a digital computer with a real-time clock. One line carried a pulse for each spike, the other a phase marker for the stimulus sinusoid. The pulse series were converted by the computer to a series of labelled event times. Lab-designed and programmed signal-processing algorithms were applied to the time series data to determine phase and transfer ratio* of afferent responses to applied stimuli as well as the regularity of the resting spike rate.

RESULTS

We intended to investigate the linear steady-state responses of anterior vertical canal and utricular afferent axons to microrotational stimuli under nearly linear

* Transfer ratio is commonly referred to as gain in studies of vestibular afferent responses. However, the term gain ideally should be used only when the transfer ratio is unitless.

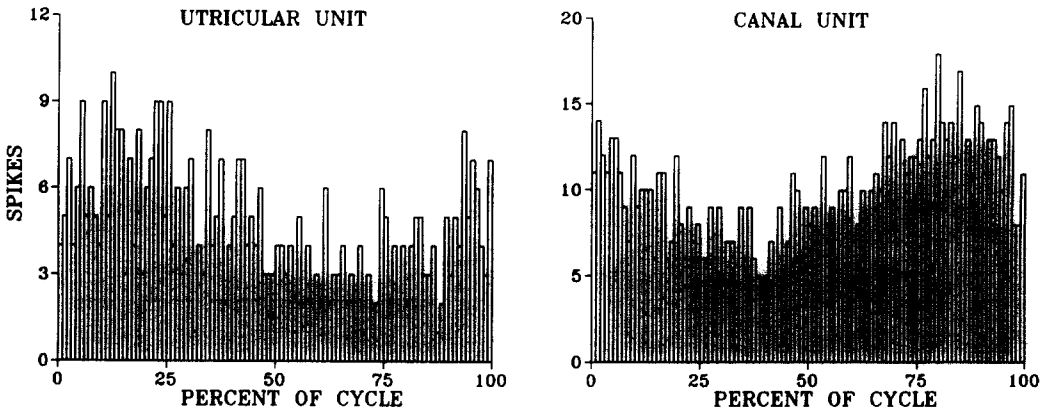

Fig. 2. Cycle histograms of 100 s of afferent spike activity in response to a 0.063 Hz, 0.4° p–p stimulus. The response peak of the modulated spike activity, in each case, was estimated by application of a Fast Fourier Transform algorithm. The result was then used to calculate transfer ratios of 21.4 and 40.5 sp/s/d/s for the utricular and canal unit respectively.

operating conditions. Thus what we hoped to obtain was modulation of the afferent axon spike rate linearly related to the stimulus amplitude. Our quest for linearity was motivated by the fact that linear response properties are by far the easiest to interpret in terms of underlying mechanisms. The desired linearity usually was achieved as long as the axon was not driven to silence during the inhibitory portion of the stimulus. Thus each unit's linear operating range was determined by its background firing rate and its transfer ratio. Generally, nearly linear responses were obtained with a stimulus amplitude of 0.4° p–p for stimulus frequencies of 0.5 Hz or less. For stimuli in the range of 1–4 Hz, reduced stimulus amplitudes (0.2–0.05° p–p) were required for linearity.

Transfer ratios

Robust, non-saturating responses were recorded for both canal and utricular afferent neurons to sinusoidal rotations in the vertical plane with peak angular accelerations as low as 0.03°/s^2 (Fig. 2). Cycle histograms for the two units with the highest transfer ratios are shown in Fig. 3. Unfortunately neither of these dye-filled axons were traceable beyond the VIIIth nerve root. Both units increased their firing rate with counter-clockwise motion around the axis of rotation shown in Fig. 1B, which does not discriminate between canal or utricular afferent neurons. The transfer ratios relative to velocity for these two units were 380 and 99 spikes/s per degree/s (sp/s/d/s).

Canal velocity transfer ratios to a 0.5 Hz stimulus (0.63°/s peak velocity) ranged from 0.4–20.7 sp/s/d/s (median = 5.0; n = 19). As shown in Fig. 4A, these transfer ratios are in general agreement with the characterization of high 'gain' canal afferent units by Honrubia et al.[7,8]. A similar plot of utricular transfer ratios versus coefficient of variation in interspike interval (CV) has a more scattered appearance (Fig. 4B). Still, the range of transfer ratios (1–40 sp/s/d/s) to a 0.5 Hz stimulus was very similar to that for canal afferent neurons. Also the majority of these utricular units had CV's greater than 0.6 as was true of the microrotationally

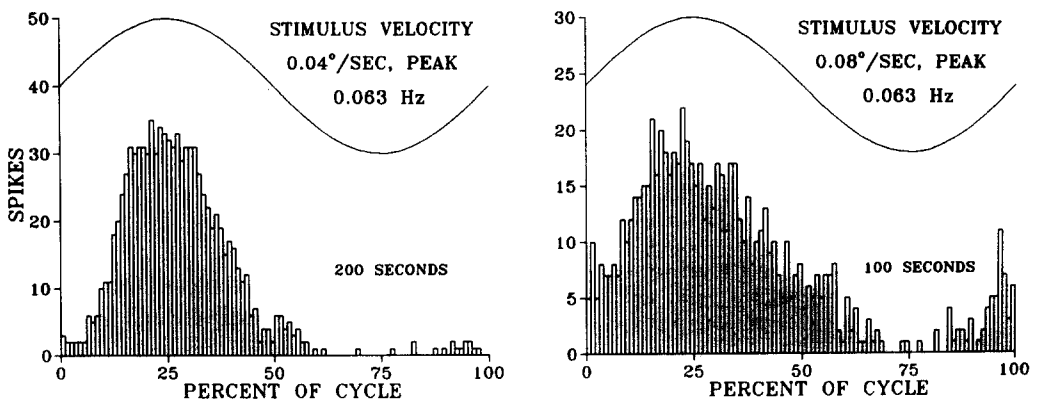

Fig. 3. Cycle histograms of the 2 units with the highest transfer ratios, peripheral origin unknown. The velocity transfer ratio of the first unit (380 sp/s/d/s) was over an order of magnitude greater than that reported previously in the literature for either canal or utricular afferent neurons.

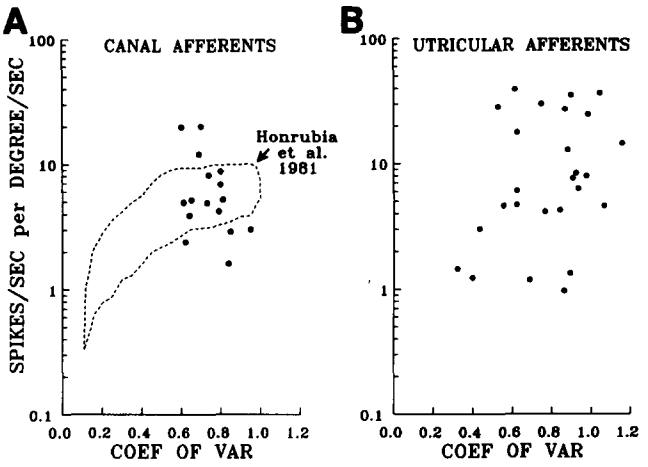

Fig. 4. A: plot of velocity transfer ratio versus coefficient of variation in the interspike interval data from 16 canal units presented with a 0.5 Hz stimulus. The dashed outline shows the range of transfer ratios reported by previous investigators. B: similar plot of data from 26 utricular units, showing a similar range of values.

TABLE I

Utricular afferent data[1]

Unit	*Velocity transfer ratio*[2]	*Mean spike rate*[3]	*Coeff. of variation*[4]	*RMS dev. ISR*[5]	*NEI (d/s)*[6]
3086	39.5	11.5	0.61	7.55	0.19
2686	36.6	8.0	1.04	15.53	0.42
3186	35.4	10.3	0.89	21.96	0.62
0386	30.0	13.6	0.75	13.68	0.46
0485	28.5	22.9	0.53	14.28	0.50
0862	27.2	6.8	0.86	10.92	0.40
0861	24.8	7.5	0.98	10.01	0.40
0385	17.8	12.0	0.62	15.13	0.85
1786	14.5	5.5	1.15	8.96	0.62
1685	12.9	7.9	0.88	9.28	0.72
9862	8.4	3.8	0.92	17.69	2.11
1785	8.0	3.6	0.97	15.10	1.90
4861	7.6	2.3	0.90	11.56	1.52
2085	6.3	4.4	0.93	14.83	2.35
0885	6.1	23.4	0.62	34.13	5.60
4862	4.7	9.1	0.62	7.28	1.54
2285	4.6	28.0	0.55	22.80	4.93
1685	4.3	6.6	0.84	16.59	3.88
0862	4.2	4.7	0.76	6.65	1.60
1185	3.0	54.4	0.43	26.86	8.90
2986	1.5	12.5	0.32	4.59	3.17
1985	1.3	3.0	0.89	5.88	4.39
9864	1.2	12.9	0.40	6.53	5.31

[1] 0.5 Hz stimulus (degrees-peak varied).
[2] sp/s/d/s.
[3] Spike rate at rest.
[4] Coefficient of variation of the interspike interval.
[5] RMS deviation of the Instantaneous Spike Rate.
[6] Noise Equivalent Input.

sensitive canal afferent units. We chose to measure the transfer ratio of utricular afferent neurons in terms of rotational velocity (rather than position) because all of the utricular units that we found to be sensitive to microrotational stimuli exhibited nearly constant velocity transfer ratios over wide ranges of frequencies.

Response data for 23 utricular units presented with a 0.5 Hz stimulus are shown in Table I. Afferent sensitivity is shown in terms of velocity transfer ratio and in terms of the Noise Equivalent Input (NEI). The NEI is the stimulus level (in degrees/second) that would evoke a spike rate response peak just equal to the Root-Mean-Square (RMS) deviation of the instantaneous resting spike rate form its mean value. Because the detectability of a stimulus-induced change in instantaneous spike rate (to any observer, including the CNS) generally will decline monotonically as the RMS deviation increases, we equate that deviation to intrinsic noise amplitude.

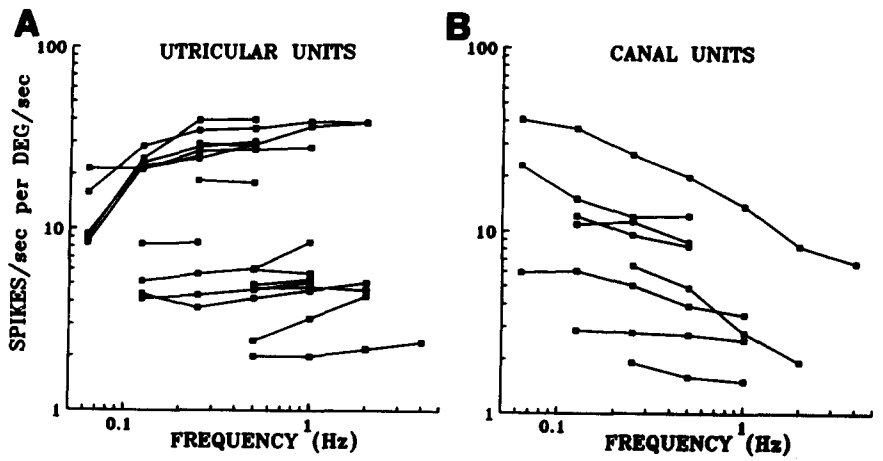

Fig. 5. A: velocity transfer ratio versus stimulus frequency for 17 utricular units showing nearly constant transfer ratios over the 0.125–4 Hz range. B: velocity transfer ratio versus stimulus frequency for 8 canal units showing a general trend of reduced response transfer ratios with increasing stimulus frequency above 0.125 Hz.

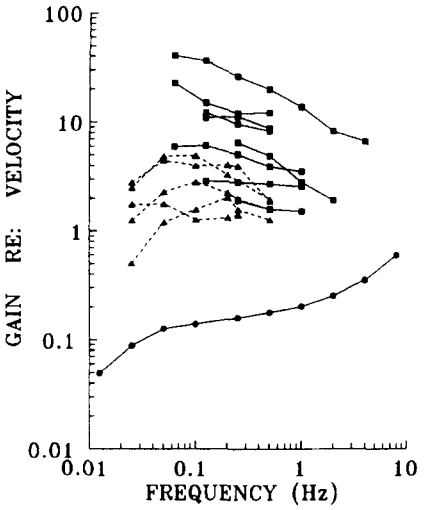

Fig. 6. Comparisons of data from Fig. 5B (squares) with bullfrog data replotted from Blanks and Precht (triangles; 1976) and mammalian data replotted from Goldberg and Fernandez (circles; 1971). Note down-sloping trend of frog canal afferent transfer ratios (all cases but one for frequencies above 0.25 Hz).

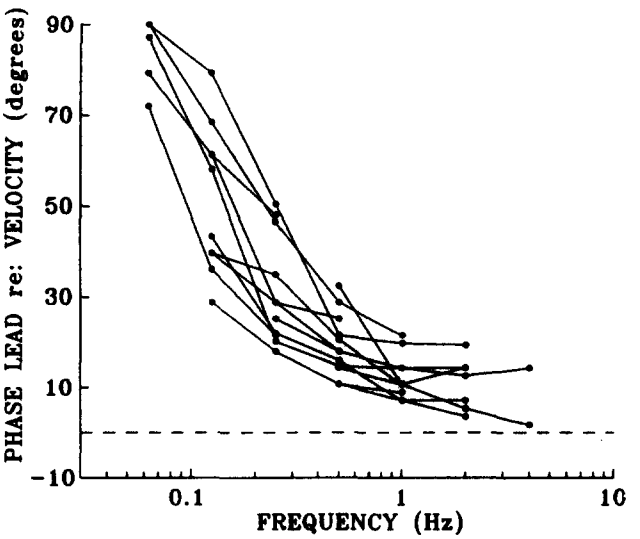

Fig. 7. Graph showing utricular afferent response phases over stimulus frequency. Note fairly stable response phase leads to frequencies above 0.5 Hz.

Frequency domain analysis

Differences between utricular and canal afferent neurons were evident in the frequency dependence of the transfer ratios. Log–log plots of the velocity transfer ratios (sp/s/d/s) vs frequency were nearly flat, with very small positive slopes, for utricular axons over the 5 octaves from 0.125–4 Hz (Fig. 5A). The plots for canal units exhibited conspicuous negative slopes over the same range of frequencies (Fig. 5B). The plotted data were taken from the 8 canal axons that were held long enough for presentation of more than two stimulus frequencies. For 3 of the axons, the slope was slightly positive over a single octave; but the trend in every case was a 4–33% (mean = 16%, S.D. = 10%) reduction in rotational velocity transfer ratio per octave above 0.125 Hz. Fig. 6 compares vertical canal data (from Fig. 5B) with data from frog horizontal canal units reported by Blanks and Precht[3]. When their data (dashed lines) are replotted in terms of sp/s/d/s, a similar tendency for down-sloping transfer ratios with frequencies above 0.1 Hz is also seen. For additional comparison, the data displayed with solid circles illustrates an example of velocity transfer ratios versus frequency for a mammalian canal afferent neuron (data replotted from Goldberg and Fernandez[6]).

Response phases

Utricular afferent response phases to peak rotational velocities < 1°/s are shown in Fig. 7. Above 0.5 Hz response phases were fairly stable with velocity phase leads of less than 20°. As the stimulus frequency was decreased below 0.5 Hz, the phase lead with respect to velocity increased, reaching nearly 90° in some units.

Four units with bimodal response phases also were

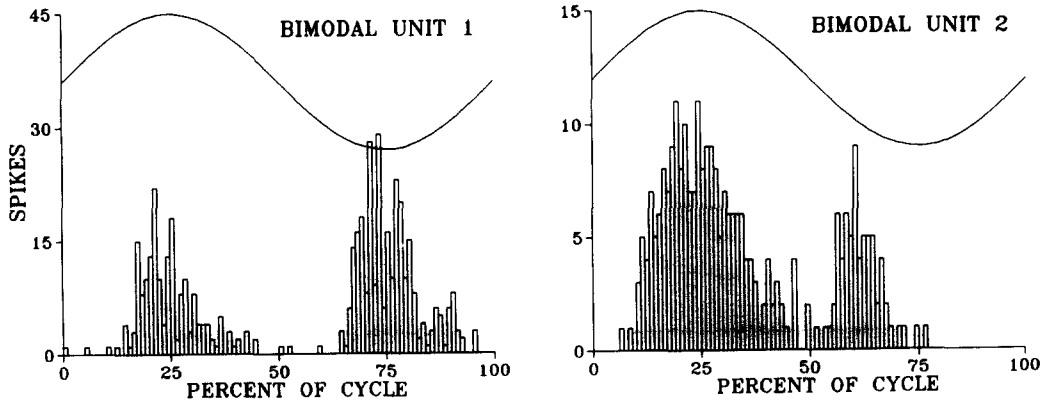

Fig. 8. Cycle histograms of 2 bimodal units presumed to innervate opposite sides of the utricular striolar reversal line of hair cell polarization. Histograms represent 100 s of data with a stimulus frequency of 0.5 Hz for unit 1 and 0.125 Hz for unit 2 (0.2° peak displacement).

encountered; but none of these were traced to their peripheral arborizations. These afferent neurons most likely innervated hair cells on opposite sides of the striolar reversal line as has been shown to occur in a previous study[2]. It is very unlikely that these bimodal responses were generated by centripetal accelerations (see Discussion). Fig. 8 illustrates the responses of two bimodal units. The response peaks of unit 1 were 180° apart, suggesting similar response dynamics of the innervated hair cells on either side of the striolar reversal line (0.5 Hz stimulus). However, this was not the case for unit 2 (0.125 Hz stimulus). At this stimulus frequency, the first peak was within 15° of the positive velocity peak, whereas the second peak lead the negative velocity peak by roughly 50°.

Anatomical correlations

Eight microrotationally sensitive canal afferent axons were successfully dye-filled and were all found to innervate the central crista ridge. Transfer ratios generally correlated with the number of hair cells innervated. Details of arborization patterns and transfer ratios of these afferent neurons are reported elsewhere in conjunction with a more thorough examination of other aspects of canal crista morphology[12].

Dye-filled utricular afferent axons (n = 12) were all found to innervate the striolar region (Fig. 9). The 4 dye-filled axons with the highest transfer ratios (25–37 sp/s/d/s; solid circles) innervated hair cells whose hair-

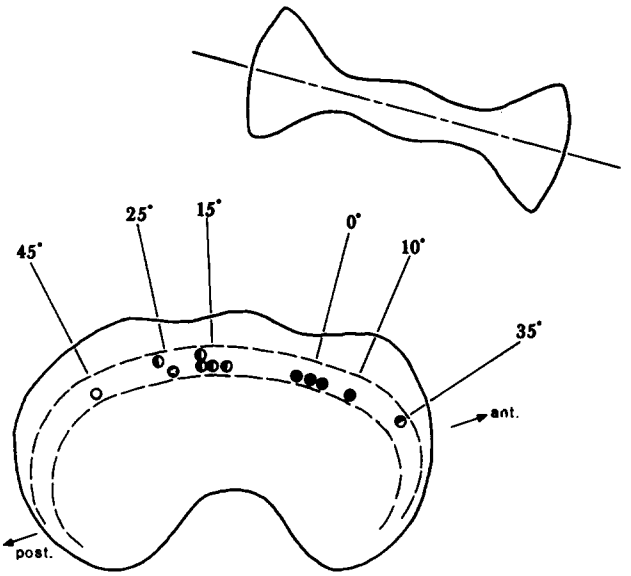

Fig. 9. Illustration showing striolar innervation of 12 successfully dye-filled utricular neurons. Solid circles represent units with high transfer ratios (25–37 sp/s/d/s); half-filled circles represent units with moderate transfer ratios (4–8 sp/s/d/s); open circles represent units with low transfer ratios (1.2 and 1.5 sp/s/d/s).

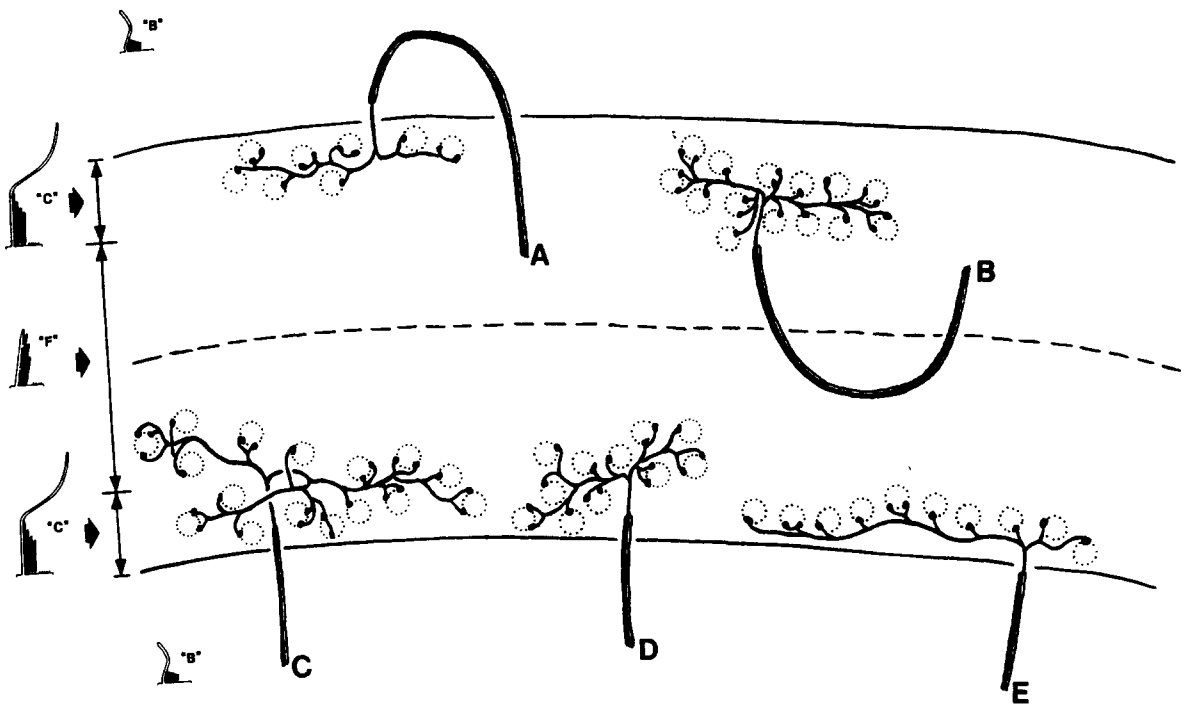

Fig. 10. Arborization patterns of 5 striolar afferent neurons with low to moderate transfer ratios (1–8 sp/s/d/s). Innervated hair cells are shown in dotted outline. Neuroepithelial boundaries of the striolar region are shown as solid lines. The dashed line is the line of reversal of hair cell polarization. (See text for discussion.)

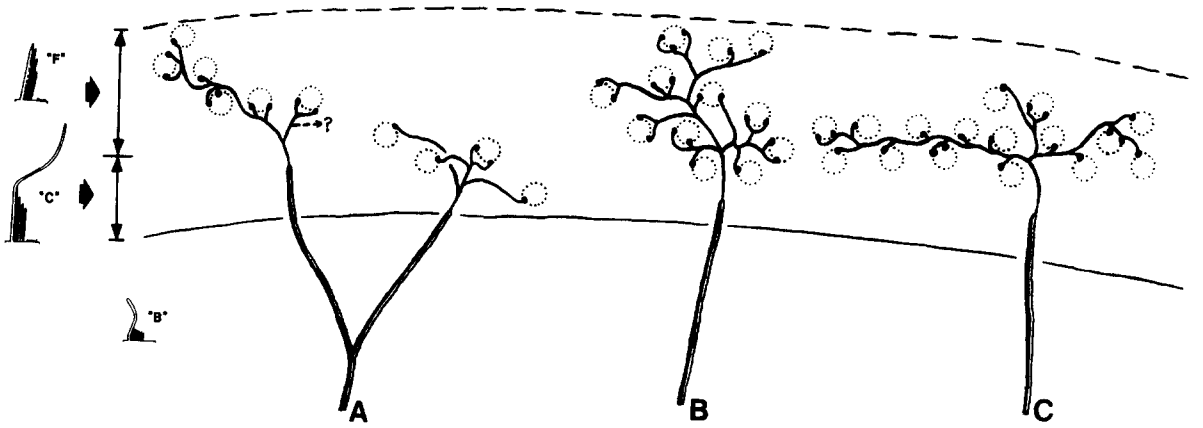

Fig. 11. Arborization patterns of 3 striolar afferent neurons with high transfer ratios (25–37 sp/s/d/s). Innervated hair cells are shown in dotted outline. Only one side of the striolar region is depicted with the solid line indicating the proximal boundary and the dashed line marking the mid-striolar reversal line of hair cell polarization. (See text for discussion.)

bundle orientations were aligned most closely with the direction of stimulus acceleration (or equivalent acceleration) component parallel to the macular plane (see Discussion). The hair bundles of the other hair cells innervated by dye-filled axons were not sufficiently misaligned with that acceleration component, however, to account for their relatively lower transfer ratios on the usual basis of a cosine function[17]. Details of utricular arbors were available for 8 of the dye-filled axons. The afferent arborizations shown in Fig. 10 were all units with lower transfer ratios (1–8 sp/s/d/s). The dashed line represents the mid-line of the striolar region. Hair cells on either side of this reversal point have kinocilia approximately the same length as the longest row of stereocilia (Type F, see ref. 9). These hair cells were shown by Baird and Lewis[2] to be more phasic in their response properties. Striolar hair cells further from the mid-line have, relatively, much longer kinocilia and were shown by the same authors to be more phasic-tonic in character (Type C). The non-striolar hair cells with tonic response properties have hair cell tufts with the appearance of scaled down phasic-tonic hair cell tufts (Type B). The afferent neurons illustrated in Fig. 10, which had lower transfer ratios, innervated a high proportion of the outer rows of striolar hair cells (i.e. phasic–tonic hair cells). Of the 4 dye-filled axons with high transfer ratios, one was not traceable beyond the point where it entered the striolar epithelium. The other 3 axons innervated a larger proportion of the more central rows of hair cells (Fig. 11) than did the afferent neurons with lower transfer ratios.

DISCUSSION

For any sensor based on seismic mass, response requires the presence of acceleration or (the equivalent acceleration of) gravity. The dynamics of the sensor may transform the response so that its amplitude over extended frequency ranges is proportional to something other than acceleration (e.g. velocity, displacement, or jerk), but without acceleration per se there would be no response at all. The utricle and semicircular canal both are presumed to be based on seismic masses (e.g. the otoconial mass in the utricle and the fluid mass in the semicircular canal). Although other components have been shown to elicit weak responses from it, the semicircular canal is far more sensitive to the rotational acceleration component aligned with the canal itself. In the experiments reported here, the amplitude of the rotational acceleration component aligned with the semicircular canal was

$$A\omega^2\cos(\omega t) \quad (1)$$

where A is the peak angular displacement of the sinusoidal tilt; ω is the frequency of the stimulus in rad/s; and t is time.

Attempts in the past to estimate vestibular 'thresholds' have suggested, that the minimum rotational acceleration detectable by the semicircular canal organs was on the order of $0.2°/s^2$. This conclusion was based on: (1) human perceptual studies, (2) the minimum acceleration for the induction of nystagmus in humans, and (3) the extrapolation of response vs amplitude plots to zero response for primary afferent neurons in the frog and central vestibular neurons in the cat (see Precht[13], for review). Lowenstein[10] and others have proposed in principle that the responsiveness of canal afferent neurons with non-zero resting spike rates should extend to zero stimulus amplitude, with no threshold; the detectability of responses would be limited by the noise in the neuron. The known limits of detectability of vestibular stimuli by the

CNS were extended by studies of the vestibulo–ocular reflex in response to very small amplitude sinusoidal rotations[15,19]. Compensatory eye movements were measurable to peak rotational accelerations of 0.04°/s^2. In the present study we have identified individual vestibular afferent neurons, in the frog, capable of responding with measurable modulations in their spike rates to comparably small accelerations.

The utricle has been shown to be selectively responsive to acceleration components parallel to the plane of its macula. The stimulus in the experiments reported here was directed along an arc that intercepted the macular plane at 90°. Consequently, there were no displacement or velocity components parallel to the macular plane; and the acceleration component parallel to that plane was centripetal on both the upward and the downward phases of the stimulus. The amplitude of the centripetal acceleration was

$$rA^2\omega^2\sin^2(\omega t) \tag{2}$$

where r is the distance between the center of rotation for the stimulus and the point at which the acceleration is measured; and A, the rotational amplitude, is given in radians. For every cycle of the sinusoidal tilt stimulus, this centripetal acceleration amplitude progressed through two full cycles. Regardless of the dynamics of the utricle itself, and the transformations imposed by them on the response, the cycle histogram of the response would be bimodal. Thus, for the majority of utricular axons, which exhibited unimodal cycle histograms, the centripetal acceleration component could not have been the effective stimulus.

The only alternative is the equivalent acceleration of gravity. The component of that acceleration parallel to the macular plane had an amplitude equal to

$$g\ \sin[A\ \cos(\omega t)] \tag{3}$$

where g is the magnitude (approx. 9.8 m/s^2) of the equivalent acceleration of gravity. For the very small values of A (peak angular rotation) used in these experiments, the amplitude of the gravitational acceleration component parallel to the macular plane was approximately

$$gA\ \cos\ (\omega t) \tag{4}$$

In response to this acceleration, the utricle would produce unimodal cycle histograms, as it did for the most part in our experiments.

The utricular units reported in this paper exhibited nearly constant rotational-velocity transfer ratios (ratio of peak response spike rate to peak stimulus rotational-velocity) over 4 or more frequency octaves above 0.1 Hz. Above their low-frequency corners and up to at least 4 Hz (the highest stimulus frequency used in this study), the log–log plots of utricular response amplitude vs frequency consistently were very close to the form

$$-K\omega\ \sin\ (\omega t) \tag{5}$$

where K is an arbitrary constant. This result implies that the utricular dynamics effectively differentiated the acceleration stimulus. In other words, the frog utricular axons from which we were recording were responding in direct proportion to jerk (rate of change of acceleration). The amplitude of the equivalent jerk derived from the rate of change of the gravitational acceleration component parallel to the macular plane was

$$-gA\omega\ \sin\ (\omega t) \tag{6}$$

The amplitude of the centripetal jerk component computed from the rotational motion (neglecting gravity) was

$$-(1/2)rA^2\omega^3\ \sin\ (2\omega t) \tag{7}$$

which would have produced bimodal cycle histograms. The ratio of peak amplitudes of centripetal and gravitational jerk components was

$$rA\omega^2/2g \tag{8}$$

which, for the 3 mm maximum value of r (see Materials and Methods) is equal approximately to

$$0.0003\ Bf^2 \tag{9}$$

where f is the stimulus frequency in Hz; and B is the peak rotational displacement in degrees. For the largest peak rotational displacement (0.4°) and the highest frequency (4 Hz) used for the utricular axons in this study, the ratio of centripetal jerk to gravitational jerk was 0.002. Thus the gravitational jerk amplitude in all cases was much greater than the centripetal jerk amplitude.

Over 4 or more octaves of stimulus frequencies, the (striolar) utricular axons in this study signaled rotational velocity. Furthermore, they did so with high transfer ratios and considerably more faithfully than did the vertical canal axons that we observed with comparable transfer ratios. This sensitivity of an otoconial organ to rotational velocity evidently arises from utricular dynamics that transform responses to acceleration into signals directly proportional to the time derivative of acceleration (jerk). This would be reflected in phasic responsive-

ness to linear acceleration itself, often seen in studies of saccular and utricular afferents[4,5,11]. It would be translated by gravity into rotational velocity sensitivity — a function normally attributed to the semicircular canals. The range of jerk sensitivities observed in the utricular axons reported here was 5.6–225 sp/s/m/s^3. The projection of the 1.0 *g* (9.8 m/s^2) gravity vector onto the utricular macula evidently translated this into rotational velocity sensitivity of 1–40 sp/s/d/s. The highest transfer ratios observed in these bullfrog utricular axons were more than an order of magnitude greater than those determined from published data on mammalian utricular afferent responses to sinusoidal tilt stimuli[1].

Transducer engineers ordinarily distinguish between the *transfer ratio* (gain) of a sensor and its *sensitivity*, with the latter taking into account the noise associated with the sensor. When there is noise in the mechanics of the input side of a sensor (e.g. in thermal motion of the hair bundle and its associated mechanical circuitry) then increasing the transfer ratio of the transduction process of subsequent stages in the sensor will increase amplification of noise as much as it increases amplification of the signal being sensed. A conventional measure of sensitivity that incorporates the impact of noise is *noise equivalent input* — defined to be the amplitude of an input signal that produces a response at the output of the sensor just equal to the total noise produced by the sensor at that point. For purposes of this paper, we have taken the noise amplitude at the output of each unit to be the RMS deviation of the instantaneous spike rate from the mean spike rate. If that deviation were zero (i.e. the resting discharge were perfectly periodic), then, in principle, even the slightest signal-induced deviation of the resting spike rate would be detectable by the central nervous system. Spontaneous (non-signal-related) deviations of the spike rate provide a noisy background that tends to hide signal-induced deviations. The final column in Table I gives the stimulus strength that would produce a response whose amplitude is just equal to the RMS deviation of the instantaneous spike rate. The units in Table I are ranked according to their velocity transfer ratio. Note that there is a strong reverse correlation in this case between the transfer ratio and this measure of noise equivalent input. This in turn suggests that much of the noise is generated after the transduction and amplification process — perhaps in the synaptic process between hair cell and primary afferent dendrite, perhaps in the primary afferent dendrite itself (prior to spike initiation). Note too that our measure of noise amplitude is not strongly correlated with the coefficient of variation of the instantaneous spike rate.

Acknowledgements. This research was supported by NASA Grant NAG 2-448.

REFERENCES

1 Anderson, J.H., Blanks, R.H.I. and Precht, W., Response characteristics of semicircular canal and otolith systems in cat. I. Dynamic responses of primary vestibular fibers, *Exp. Brain Res.*, 32 (1978) 491–507.

2 Baird, R.A. and Lewis, E.R., Correspondences between afferent innervation patterns and response dynamics in the bullfrog utricle and lagena, *Brain Research*, 369 (1986) 48–64.

3 Blanks, R.H.I. and Precht, W., Functional characterization of primary vestibular afferents in the frog, *Exp. Brain Res.*, 25 (1976) 369–390.

4 Fernandez, C. and Goldberg, J.M., Physiology of peripheral neurons innervating otolith organs of the squirrel monkey. III. Response dynamics, *J. Neurophysiol.*, 39 (1976) 996–1008.

5 Goldberg, J.M. and Fernandez, C., Vestibular mechanisms, *Annu. Rev. Physiol.*, 37 (1975) 129–162.

6 Goldberg, J.M. and Fernandez, C., Physiology of peripheral neurons innervating semicircular canals of the squirrel monkey. III. Variations among units in their discharge properties, *J. Neurophysiol.*, 34 (1971) 676–684.

7 Honrubia, V., Sitko, S., Kimm, J., Betts, W. and Schwartz, I., Physiological and anatomical characteristics of primary vestibular afferent neurons in the bullfrog, *Int. J. Neurosci.*, 15 (1981) 197–206.

8 Honrubia, V., Hoffman, L., Sitko, S. and Schwartz, I.R., Anatomic and physiological correlates in bullfrog vestibular nerve, *J. Neurophysiol.*, 61 (1989) 688–701.

9 Lewis, E.R. and Li, C.W., Hair cell types and distributions in the otolithic and auditory organs of the bullfrog, *Brain Research*, 83 (1975) 35–50.

10 Lowenstein, O., Peripheral mechanisms of equilibrium, *Br. Med. Bull.*, 12 (1956) 114–118.

11 Macadar, O., Wolf, G.E., O'Leary, D.P. and Segundo, J.P., Response of the elasmobranch utricle to maintained spatial orientation, transitions and jitter, *Exp. Brain Res.*, 22 (1975) 1–12.

12 Myers, S.F. and Lewis, E.R., Hair cell tufts and afferent innervation of the bullfrog crista ampullaris, *Brain Research*, in press.

13 Precht, W., The physiology of the vestibular nuclei. In H.H. Kornhuber (Ed.), *Handbook of Sensory Physiology Vol. VI/2, Vestibular System, Part 1 Basic Mechanisms*, Springer New York, 1974, pp. 353–416.

14 Precht, W., Llinas, R. and Clarke, M., Physiological responses of frog vestibular fibers to horizontal angular rotation, *Exp. Brain Res.*, 13 (1971) 378–407.

15 Skavenski, A.A., Hansen, R.M., Steinman, R.M. and Winterson, B.J., Quality of retinal image stabilization during small natural and artificial body rotations in man, *Vision Res.*, 19 (1979) 675–683.

16 Shimazu, H. and Precht, W., Tonic and kinetic responses of cat's vestibular neurons to horizontal angular acceleration, *J. Neurophysiol.*, 28 (1965) 991–1013.

17 Shotwell, S.L., Jacobs, R., Hudspeth, Aj., Directional sensitivity of individual vertebrate hair cells to controlled deflection of their hair bundles, *N.Y. Acad. Sci.*, 1981:1–10.

18 Stewart, W.W., Functional connections between cells as revealed by dye-coupling with a highly fluorescent naphthalamide tracer, *Cell*, 14 (1978) 741–759.

19 Winterson, B.J., Collewijn, H. and Steinman, R.M., Compensatory eye movements to miniature rotations in the rabbit: implications for retinal image stability, *Vision Res.*, 19 (1979) 1155–1159.